Controlling spin waves by inhomogeneous spin-transfer torques

Lorenzo Gnoatto,[1,*] Jean F. O. da Silva,[2] Artim L. Bassant,[3] Rai M. Menezes,[2,4] Rembert A. Duine,[1,3] Milorad V. Milošević,[2,†] and Reinoud Lavrijsen[1]

[1]*Department of Applied Physics and Science Education, Eindhoven University of Technology, P.O. BOX 5132, 5600 MB Eindhoven, Netherlands*

[2]*COMMIT, Department of Physics, University of Antwerp, Groenenborgerlaan 171, B-2020 Antwerp, Belgium*

[3]*Institute for Theoretical Physics, Utrecht University, Princetonplein 5, 3584 CC Utrecht, Netherlands*

[4]*Departamento de Física, Universidade Federal de Pernambuco, Cidade Universitária, 50670-901 Recife-PE, Brazil*

(Received 1 October 2025; accepted 5 March 2026; published 10 April 2026)

We investigate the interplay between spin currents and spin waves in nanofabricated Permalloy waveguides with geometrical constrictions. Using propagating spin-wave spectroscopy, micromagnetic simulations, and analytical modeling, we provide experimental evidence that spin-wave phase can be modulated by inhomogeneous spin-transfer torques generated by current-density gradients shaped by the constriction geometry. Narrower constrictions enhance these gradients and modify the internal field for Damon–Eshbach spin waves, resulting in pronounced changes in spin-wave group velocity and phase. We show a quantitative experimental demonstration of deterministic spin-wave phase modulation enabled by geometry-engineered nonuniform spin-transfer torques. Beyond enabling a scalable route to magnonic interferometry—a building block for spin-wave-based computing—our findings establish a platform to control spin-wave dynamics in spatially varying current landscapes, relevant for analog-gravity experiments in condensed matter systems.

DOI: 10.1103/lr39-lgtx

I. INTRODUCTION

The interaction between spin-polarized currents and magnons has emerged as a powerful mechanism for manipulating spin waves (SWs) in magnonic systems. This coupling, mediated by spin-transfer torque (STT) [1], enables control over SW amplitude [2], frequency [3], and, as in this work, phase. Early theoretical and experimental studies [1,4,5] focused on uniform direct currents, revealing effects such as the spin-wave Doppler shift [3] and establishing the foundations of STT physics [6,7]. In this context, SW magnetization dynamics is subjected to an STT-induced frequency shift given by $\Delta\omega_{\mathrm{STT}} = -v_{\mathrm{d}}k$ [3], where the spin-polarized electron drift velocity is $v_{\mathrm{d}} = gP\mu_{\mathrm{B}}J/(2|e|M_{\mathrm{s}})$ and k is the wavevector. Here, g is the Landé g factor, P the spin polarization, μ_{B} the Bohr magneton, e the elementary charge, M_{s} the saturation magnetization, k the wavevector, and J the current density—explicitly showing the direct proportionality between STT effects and J. Note that the use of spin-orbit-torques (SOTs) [2,8] has also been explored but in first order does not lead to "doppler shifts" as is the aim of our work. In the present work, "inhomogeneous STT" refers specifically to spatial variations of the current density $J(x)$ imposed by the constriction geometry, which lead to a spatially varying spin drift velocity $v_d(x)$ and therefore a position-dependent STT-induced phase accumulation along the spin-wave propagation path.

SWs are dispersive waves whose properties are defined by their dispersion relation $\omega(k)$, which links frequency, wavevector, and other magnetic parameters such as saturation magnetization, externally applied magnetic field and effective field [9,10]. Their group velocity, $v_{\mathrm{g}} = \partial\omega/\partial k$, sets the speed at which energy and information are transported by the wavepacket, while the phase velocity, $v_{\mathrm{p}} = \omega/k$, corresponds to the speed of an individual spectral component. Since STT modifies the dispersion, it can affect both v_{g} and v_{p}, with v_g maximized when the electron flow and wavevector are codirected. This dual control forms the basis for the STT-driven phase-modulation effects investigated experimentally and theoretically in this work.

Phase modulation enabled by spatially varying spin-polarized currents, could serve as a building block for interferometric devices such as Mach–Zehnder-type spin-wave interferometers [11,12]. However, practical implementations remain limited, and the influence of spatially varying spin-polarized currents on propagating SWs is not fully understood. It has been previously shown theoretically that inhomogeneous currents can give rise to exotic dynamical regimes, including magnonic analogues of black holes [13] and spin-wave lasing [14,15], in regimes where the spin-drift velocity (v_d) exceeds the spin-wave group velocity (v_g). While those works focused on extreme transport conditions, the present study addresses a related, but less explored, question: How current density gradients, even in the linear regime,

*Contact author: l.g.gnoatto@tue.nl

†Contact author: milorad.milosevic@uantwerpen.be

Published by the American Physical Society under the terms of the Creative Commons Attribution 4.0 International license. Further distribution of this work must maintain attribution to the author(s) and the published article's title, journal citation, and DOI.

influence spin-wave propagation and phase. Understanding this regime is essential for realizing analog gravity scenarios in magnetic systems, where smooth variations in v_d play the role analogous to spacetime curvature [13].

Experimental studies on inhomogeneous current transport have largely focused on spin-Hall nano-oscillators [16], where current gradients modulate local magnetization dynamics [17]. Yet, their impact on the propagation of spin waves in extended metallic ferromagnets remains comparatively less explored experimentally in extended metallic ferromagnetic waveguides. In this work, we demonstrate that geometric constrictions, i.e., the cross section of a Permalloy waveguide strip varies with position leading to a position dependent current density, which in its turn produces a gradient in the STT-induced spin-wave phase modulation via the inhomogeneous STT. Using propagating spin-wave spectroscopy (PSWS) [18,19], micromagnetic simulations, and analytical modeling, we show that phase accumulation is highly sensitive to constriction geometry, providing a pathway toward controlling spin-wave interference in reconfigurable magnonic circuits.

II. METHODS

To probe the impact of inhomogeneous STT on spin-wave transport, PSWS offers access to the frequency [3], amplitude [2], and phase response [20] of spin waves with high precision between two points along a spin-wave conduit. Being inherently a two-port measurement [19], PSWS probes the cumulative effect of spin-wave propagation between the excitation and detection antennas. The devices consist of 2-μm-wide Permalloy microstrips, fabricated as described in Ref. [21], with a Ta(4)/Py(20)/Ta(4) layer stack (thicknesses in nanometers). Figure 1(a) shows a wide-field optical microscope image of a typical PSWS device. To introduce a spatially varying current density, we patterned a central constriction of width w_c between the two antennas, using $w_c =$ 2000, 1427, 1140, 857, 571, and 285 nm. These values correspond to the nominal widths defined in the lithography design and were arbitrarily chosen. The length (l) of the tapered section was kept constant at 4.5 μm for all devices. Samples with $w_c < 2000$ nm are referred to as constricted samples. A scanning electron microscope image of the central region is shown in Fig. 1(b), indicating the width variation and the directions of spin-wave propagation and applied DC current.

Based on previous experimental studies [22,23], variations in the internal effective field near geometrical constrictions—driven by demagnetization effects—can significantly impact spin-wave propagation. To investigate this and ensure proper spin-wave (SW) transmission, crucial for their detection and subsequent characterization with applied current, we first performed PSWS measurements in the absence of current, sweeping the excitation frequency from 4 to 13 GHz under a fixed external magnetic field.

III. RESULTS: PSWS WITHOUT CURRENT

Representative transmitted spectra for a device with $w_c =$ 571 nm are shown in Fig. 1(c), displaying the real, imaginary, magnitude, and phase components of the signal. The real and

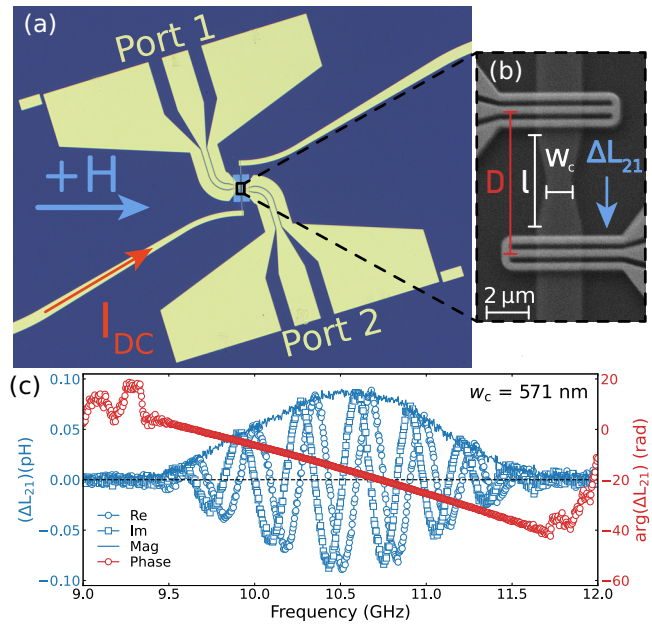


FIG. 1. (a) Optical microscope image of the PSWS device, showing the orientations of the applied DC current (I_{DC}) and the external magnetic field (H). (b) Scanning electron microscope image of the antenna region and ferromagnetic strip, featuring a constriction with width $w_c = 1140$ nm, constriction total tapered length $l = 4.5$ μm and antenna distance center to center D = 6.1 μm. (c) Example mutual inductance spectra for a device with $w_c = 571$ nm, showing the real, imaginary, and magnitude components of the signal, as well as the corresponding phase (right axis), measured at $\mu_0 H = +100$ mT.

imaginary parts exhibit the oscillatory behavior characteristic of spin-wave phase accumulation between antennas separated by a distance D [19]. The phase signal varies linearly with frequency within the transmission band and appears noisy outside resonance, consistent with expectations for a dispersive medium. This linear frequency dependence arises because SWs excited at different frequencies propagate at different phase velocities—unlike in nondispersive media such as light in vacuum, where phase remains constant across frequencies. Notably, this phase behavior also encodes information about the group velocity, which can be extracted by analyzing the frequency-dependent phase accumulation, as discussed later.

To understand how geometrical constrictions influence spin-wave propagation, we first extract the dispersion relations for both a reference (unconstricted) strip and a constricted device. As discussed earlier, demagnetization effects in narrow geometries locally modify the internal effective field, potentially suppressing spin-wave transmission at low external fields [22,23]. Figures 2(a) and 2(b) show the experimentally measured dispersions for the reference and $w_c =$ 571 nm waveguides, respectively. In the wide device, spin waves are supported down to lower external fields, while in the constricted geometry, a threshold field is required before spin-wave propagation becomes visible. This confirms that the constriction acts as a magnetic barrier for spin waves, and that sufficiently strong external fields are needed to overcome the local demagnetizing effects and enable spin-wave guiding. To further support our interpretation,

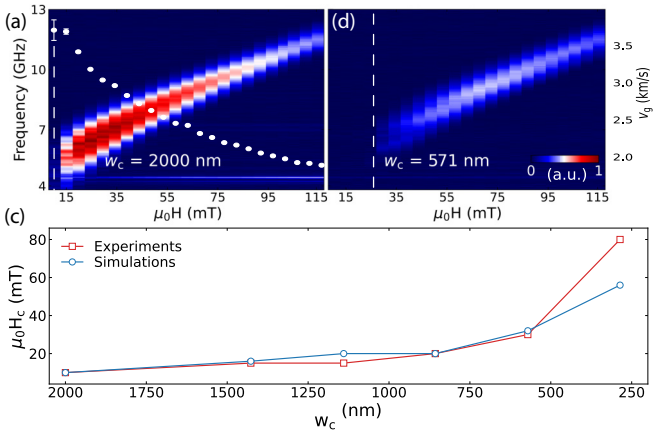


FIG. 2. Transmitted spin-wave spectra (mutual inductance amplitude) for (a) a uniform waveguide ($w_c = 2000$ nm) and (b) a constricted waveguide ($w_c = 571$ nm). The dots in (a) represent the extracted group velocity, plotted using the right-hand axis shown in (b) for clarity. (c) Minimum applied magnetic field required for detectable spin-wave transmission, plotted as a function of constriction width.

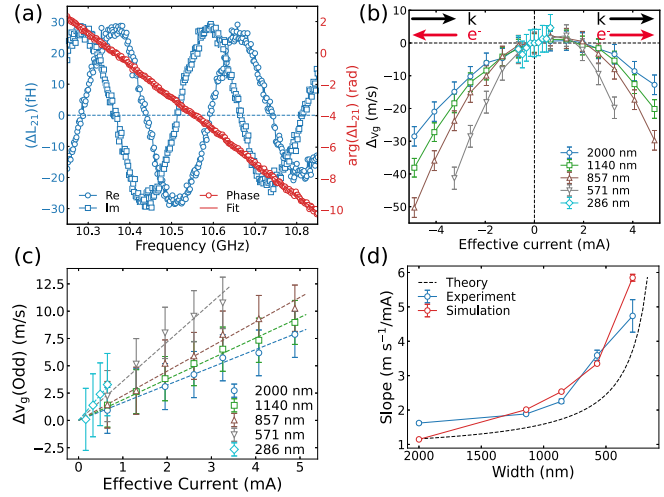


FIG. 3. (a) Real, imaginary, and phase components of the mutual inductance for the sample with $w_c = 286$ nm at $I \approx 0.6$ mA (the noisiest dataset). (b) Absolute change in group velocity, $\Delta v_g = v_g(I) - v_g(0)$, as a function of effective current for various constriction widths. Arrows indicate the relative directions of electron flow (e^-) and spin-wave propagation (k). (c) Antisymmetric component of the relative group velocity change, with linear fits shown as dashed lines. (d) Slopes of the experimental data fits in (c), from simulations and coefficient of Eq. (1) with $M_s = 750$ kA, $P = 0.55$, $g = 2.19$, $l = 4.5$ μm, $D = 6.1$ μm, and $w_0 = 2000$ nm highlighting the dominant current-induced contribution to Δv_g for narrower constrictions (see Supplemental Material [24] for details on simulated slopes and P value extraction).

we performed micromagnetic simulations under comparable conditions (see Supplemental Material [24] for details on simulations), which reproduce the experimental dispersions and the effect of the constriction.

Figure 2(c) summarizes the minimum magnetic field required for detectable spin-wave transmission ($\mu_0 H_c$), extracted from both experiments and simulations as a function of the constriction width w_c. Experiment and simulation are in excellent agreement, confirming that demagnetization effects set the threshold field for spin-wave propagation. In narrow constrictions, demagnetization induces a slight canting of the magnetization near the constriction, which, although small relative to the saturation magnetization, leads to partial reflection of spin waves. In contrast, wider constrictions confine this canting to the edges, allowing Damon-Eshbach mode propagation through the central region. As the external field is increased, the magnetization becomes more uniform, reducing demagnetization effects and enabling transmission through narrower constrictions. At low fields, however, suppressed magnetic ordering near the constriction inhibits the propagation of magnetostatic surface waves, effectively creating a transmission stop band [25].

IV. RESULTS: PSWS WITH CURRENT

As introduced, in a uniform current density distribution, v_g increases when the spin-polarized electron flow and the wavevector are parallel, because of the uniform STT acting along the propagation path. In a nonuniform current density distribution—such as that created by a constriction—this effect is expected to be amplified, as regions of higher current density locally enhance the STT, leading to stronger modulation of the spin-wave group velocity. To test this hypothesis, we applied a DC current to devices with different constriction widths, focusing on the accumulated phase and the resulting group velocity, v_g. Figure 3(a) shows the real and imaginary components of the measured spectra, together with the extracted phase for a representative sample under applied current. The group velocity is obtained by first calculating the group delay time, $\tau_g(\omega) = -\frac{d\phi(\omega)}{d\omega}$, which represents the time taken by the wavepacket envelope to travel from the input to the output antenna, where $\phi(\omega)$ is the phase as a function of frequency. Knowing the propagation distance ($D = 6.1$ μm in our experiments), and following the procedure of Ref. [26], we extract the group velocity as $v_g = \frac{\partial\omega}{\partial k} = \frac{D}{\tau_g}$.

This method was also used to extract v_g for the wide strip, with the results shown on Fig. 2(a). The obtained values are in excellent agreement with previously reported group velocities in Permalloy microstrips [27]. To be able to characterize samples with narrower constriction (e.g., $w_c = 286$ nm), we apply an external magnetic field of $\mu_0 H = 100$ mT to minimize demagnetizing effects and ensure efficient SW transmission (see Supplemental Material [24] for SWs amplitude data).

Figure 3(b) shows the group velocity variation as a function of effective current, assuming 95% current flow through the ferromagnetic layer owing to shunting effects of seeding and capping layers [21]. For small currents, the response is linear, transitioning to a nonlinear regime at higher currents. We attribute this behavior to two primary contributions: a quadratic component resulting from Joule heating [2,28], and a linear Doppler-like term arising from the spin-drift velocity v_d [3].

To model the interaction between SWs and nonuniform current distributions, we performed micromagnetic calculations in comparable conditions, where Poisson solver for the current distribution was implemented within the mumax[3]

simulation platform [29]. Details on the implementation can be found in Ref. [30] and the Supplemental Material [24]. All experiments and simulations are performed at $\mu_0 H = 100\,\mathrm{mT}$, where the magnetization is saturated and demagnetizing effects are minimized, as previously discussed.

To interpret the linear regime observed at small currents in Fig. 3(b), we developed an analytical model based on the spatially varying spin-wave phase induced by the current gradient. Under the assumption of weak damping and adiabatic propagation, we obtain the following expression for the relative change in group velocity:

$$\Delta v_g = v_d\left(1 + \frac{l}{2D}\left(\frac{w_0}{w_c} - 1\right)\right), \tag{1}$$

where l is the length of the constriction and w_0 the initial width. A detailed derivation, including the effects of finite antenna width, smooth current profiles, and Joule heating, is provided in the Supplemental Material [24].

To better isolate current-induced effects from quadratic Joule heating and facilitate direct comparison with simulations and theory, Fig. 3(c) shows the odd component of the group velocity variation, defined as $\Delta v_{g(\mathrm{odd})} = (\Delta v_g(+I) - \Delta v_g(-I))/2$, for devices with and without constrictions. As expected, narrower constrictions result in larger group velocity modulation for a given current, as the SWs will experience an effective larger current density while they travel between the antennas. In Fig. 3(d), we plot the slope of the experimental curves from Fig. 3(c), together with the corresponding values obtained from micromagnetic simulations that account for realistic, nonuniform current density distributions (see Supplemental Material [24] for details). These are compared with the theoretical scaling predicted by Eq. (1). The agreement across experiment, simulation, and theory confirms the geometric dependence of the spin-wave response to spin-polarized current gradients. While separating all individual contributions via dedicated simulations is an interesting direction for future work, the present experimental scaling with constriction geometry and current polarity provides strong evidence for a dominant current-driven torque contribution.

V. CONCLUSION

In summary, we have shown that inhomogeneous spin-transfer torques, engineered through simple geometrical constrictions, enable deterministic control of the phase and group velocity of propagating spin waves. Our combined experimental, numerical, and analytical analysis demonstrates that current-induced gradients directly modulate the dispersion, providing a scalable route to phase control under fixed applied current. This functionality establishes a foundation for reconfigurable wave-based devices such as magnonic interferometers, while also offering an experimental pathway toward analog-gravity phenomena in magnetic systems, where spatially varying spin-drift velocities emulate curved spacetime.

ACKNOWLEDGMENTS

We thank Bert Koopmans for valuable discussions. This work was supported by the Dutch Research Council (NWO), the Research Foundation-Flanders (FWO), and the Special Research Funds of the University of Antwerp (BOF-UA). The computational resources used in this work were provided by the VSC (Flemish Supercomputer Center), funded by Research Foundation-Flanders (FWO) and the Flemish Government – Department EWI.

DATA AVAILABILITY

The data that support the findings of this article are not publicly available. The data are available from the authors upon reasonable request.

[1] J. Slonczewski, Current-driven excitation of magnetic multilayers, J. Magn. Magn. Mater. **159**, L1 (1996).

[2] O. Gladii, M. Collet, K. Garcia-Hernandez, C. Cheng, S. Xavier, P. Bortolotti, V. Cros, Y. Henry, J.-V. Kim, A. Anane, *et al.*, Spin wave amplification using the spin Hall effect in permalloy/platinum bilayers, Appl. Phys. Lett. **108**, 202407 (2016).

[3] V. Vlaminck and M. Bailleul, Current-induced spin-wave doppler shift, Science **322**, 410 (2008).

[4] L. Berger, Emission of spin waves by a magnetic multilayer traversed by a current, Phys. Rev. B **54**, 9353 (1996).

[5] M. Stiles and J. Miltat, Spin transfer torque and dynamics, in *Spin Dynamics in Confined Magnetic Structures III*, Topics in Applied Physics, Vol. 101 (Springer, Berlin, 2006).

[6] Z. Li and S. Zhang, Domain-wall dynamics driven by adiabatic spin-transfer torques, Phys. Rev. B **70**, 024417 (2004).

[7] S. Zhang and Z. Li, Roles of nonequilibrium conduction electrons on the magnetization dynamics of ferromagnets, Phys. Rev. Lett. **93**, 127204 (2004).

[8] J. S. Harms, H. Y. Yuan, and R. A. Duine, Enhanced magnon spin current using the bosonic Klein paradox, Phys. Rev. Appl. **18**, 064026 (2022).

[9] A. Mahmoud, F. Ciubotaru, F. Vanderveken, A. V. Chumak, S. Hamdioui, C. Adelmann, and S. Cotofana, Introduction to spin wave computing, J. Appl. Phys. **128**, 161101 (2020).

[10] P. Pirro, V. I. Vasyuchka, A. A. Serga, and B. Hillebrands, Advances in coherent magnonics, Nat. Rev. Mater. **6**, 1114 (2021).

[11] K.-S. Lee and S.-K. Kim, Conceptual design of spin wave logic gates based on a Mach–Zehnder-type spin wave interferometer for universal logic functions, J. Appl. Phys. **104**, 053909 (2008).

[12] T. Schneider, A. A. Serga, B. Leven, B. Hillebrands, R. L. Stamps, and M. P. Kostylev, Realization of spin-wave logic gates, Appl. Phys. Lett. **92**, 022505 (2008).

[13] A. Roldán-Molina, A. S. Nunez, and R. A. Duine, Magnonic black holes, Phys. Rev. Lett. **118**, 061301 (2017).

[14] R. J. Doornenbal, A. Roldán-Molina, A. S. Nunez, and R. A. Duine, Spin-wave amplification and lasing driven by inhomogeneous spin-transfer torques, Phys. Rev. Lett. **122**, 037203 (2019).

[15] K. Nakayama, K. Kasahara, T. Inada, and S. Tomita, Resonant amplification of spin waves with analogue black-hole horizons, Phys. Rev. Appl. **22**, 064086 (2024).

[16] V. E. Demidov, S. Urazhdin, A. Zholud, A. V. Sadovnikov, and S. O. Demokritov, Nanoconstriction-based spin-Hall nano-oscillator, Appl. Phys. Lett. **105**, 172410 (2014).

[17] V. E. Demidov, S. Urazhdin, G. De Loubens, O. Klein, V. Cros, A. Anane, and S. O. Demokritov, Magnetization oscillations and waves driven by pure spin currents, Phys. Rep. **673**, 1 (2017).

[18] J. Lucassen, C. F. Schippers, L. Rutten, R. A. Duine, H. J. Swagten, B. Koopmans, and R. Lavrijsen, Optimizing propagating spin wave spectroscopy, Appl. Phys. Lett. **115**, 012403 (2019).

[19] V. Vlaminck and M. Bailleul, Spin-wave transduction at the submicrometer scale: Experiment and modeling, Phys. Rev. B **81**, 014425 (2010).

[20] C. Weiss, M. Grassi, Y. Roussigné, A. Stashkevich, T. Schefer, J. Robert, M. Bailleul, and M. Kostylev, Excitation and reception of magnetostatic surface spin waves in thin conducting ferromagnetic films by coplanar microwave antennas. Part II: Experiment, J. Magn. Magn. Mater. **565**, 170002 (2023).

[21] L. Gnoatto, T. Molier, J. J. Lamberts, A. L. Bassant, C. F. Schippers, R. A. Duine, and R. Lavrijsen, Investigating the interplay between spin polarization and magnetic damping in $Co_xFe_{80-x}B_{20}$ for magnonics applications, Appl. Phys. Lett. **126**, 072402 (2025).

[22] V. E. Demidov, J. Jersch, S. O. Demokritov, K. Rott, P. Krzysteczko, and G. Reiss, Transformation of propagating spin-wave modes in microscopic waveguides with variable width, Phys. Rev. B **79**, 054417 (2009).

[23] V. E. Demidov, M. P. Kostylev, K. Rott, J. Münchenberger, G. Reiss, and S. O. Demokritov, Excitation of short-wavelength spin waves in magnonic waveguides, Appl. Phys. Lett. **99**, 082507 (2011).

[24] See Supplemental Material at http://link.aps.org/supplemental/10.1103/lr39-lgtx for further details on the experimental, simulation, and theoretical frameworks.

[25] F. Vilsmeier, C. Riedel, and C. H. Back, Spatial control of hybridization-induced spin-wave transmission stop band, Appl. Phys. Lett. **124**, 132407 (2024).

[26] C. Weiss, M. Bailleul, and M. Kostylev, Excitation and reception of magnetostatic surface spin waves in thin conducting ferromagnetic films by coplanar microwave antennas. Part I: Theory, J. Magn. Magn. Mater. **565**, 170103 (2023).

[27] M. Haidar, Role of surfaces in magnetization dynamics and spin-polarized transport, Ph.D. thesis, Université de Strasbourg, 2012.

[28] O. Gladii, Spin wave propagation and its modification by an electrical current in Py/Al2O3, Py/Pt and Fe/MgO films, Ph.D. thesis, Université de Strasbourg, 2016.

[29] J. Leliaert, M. Dvornik, J. Mulkers, J. D. Clercq, M. V. Milošević, and B. V. Waeyenberge, Fast micromagnetic simulations on GPU—Recent advances made with mumax^3, J. Phys. D **51**, 123002 (2018).

[30] R. M. Menezes, J. Mulkers, C. C. de Souza Silva, B. Van Waeyenberge, and M. V. Milošević, Toward magnonic logic and neuromorphic computing: Controlling spin waves by spin-polarized current, Phys. Rev. Appl. **22**, 054056 (2024).